

ORIGINAL ARTICLE

Studying the Progression of Amyloid Pathology and Its Therapy Using Translational Longitudinal Model of Accumulation and Distribution of Amyloid Beta

Tatiana Karelina^{1*}, Oleg Demin Jr¹, Oleg Demin¹, Sridhar Duvvuri² and Timothy Nicholas³

Long-term effects of amyloid targeted therapy can be studied using a mechanistic translational model of amyloid beta ($A\beta$) distribution and aggregation calibrated on published data in mouse and human species. Alzheimer disease (AD) pathology is modeled utilizing age-dependent pathological evolution for rate constants and several variants of explicit functions for $A\beta$ toxicity influencing cognitive outcomes (Adas-cog). Preventive $A\beta$ targeted therapies were simulated to minimize the $A\beta$ difference from healthy physiological levels. Therapeutic targeted simulations provided similar predictions for mouse and human studies. Our model predicts that: (1) at least 1 year (2 years for preclinical AD) of treatment is needed to observe cognitive effects; (2) under the hypothesis with functional importance of $A\beta$, a 15% decrease in $A\beta$ (using an imaging biomarker) is related to 15–20% cognition improvement by immunotherapy. Despite negative outcomes in clinical trials, $A\beta$ continues to remain a prospective target demanding careful assessment of mechanistic effect and duration of trial design.

CPT Pharmacometrics Syst. Pharmacol. (2017) 6, 676–685; doi:10.1002/psp4.12249; published online 28 September 2017.

Study Highlights

WHAT IS THE CURRENT KNOWLEDGE ON THE TOPIC?

Multiple clinical trials targeting amyloid, the hallmark of AD pathology, have failed. The key efficacy markers are CSF amyloid and brain PET, whereas neither clear correlations between them and cognitive scores have been proven nor quantification of amyloid toxic effect proposed.

WHAT QUESTION DOES THIS STUDY ADDRESS?

The questions this study address are (1) whether a mechanistic translational model can allow for prediction of long-term clinical trials and (2) what efficacy on cognition would be demonstrated under different amyloid toxicity hypotheses.

WHAT THIS STUDY ADDS TO OUR KNOWLEDGE

The mechanistic model allows for prediction as to whether long-term therapy leads to normalization of amyloid levels in different compartments. Quantitative formulation of toxicity hypotheses allows for using the trial results for hypothesis testing.

HOW MIGHT THIS CHANGE DRUG DISCOVERY, DEVELOPMENT, AND/OR THERAPEUTICS?

Our model, validated on multiple pathology progression data, allows for more comprehensive design of clinical trials. Variants of scenarios can be analyzed depending on the disease stage and type of therapy and optimized for higher efficacy and safety.

Alzheimer disease (AD) leading to the decrement of cognitive functions is hypothesized to be caused by abnormal accumulation of amyloid beta ($A\beta$) peptide,¹ which is found in soluble and insoluble forms in the postmortem brains of subjects with AD. Two peptide variants, $A\beta_{40}$ and $A\beta_{42}$, produced from amyloid precursor protein (APP), form oligomers and polymer chains,² which differ by physicochemical properties, including solubility. The brain levels of soluble and insoluble forms of $A\beta$ are distinguished in subjects with AD with respect to healthy individuals.³ Main techniques to observe the progression of amyloid pathology are the measurement of $A\beta$ changes in cerebrospinal fluid (CSF), which is used as a reference for changes in brain interstitial fluid (BIF), and positron emission tomography (PET) with $A\beta$ -specific tracers (e.g., PiB), quantifying the insoluble amyloid in brain. PET data demonstrate an increase of insoluble amyloid, whereas CSF $A\beta_{42}$ concentration is decreased,⁴

hypothetically due to the absorption of free $A\beta$ into insoluble plaques. As AD progresses, the insoluble $A\beta$ forms seem to reach a steady-state value.⁵ Soluble and insoluble amyloid neurotoxicity^{6–8} has been explored *in vitro*.⁹ Nucleation-dependent polymerization was shown to be required for neurotoxicity,¹⁰ and clinical studies reveal correlation between amyloid imaging load registered by PET and cognitive function (Adas-cog score¹¹). Although controversial results have been reported,¹² postmortem soluble amyloid correlated highly with disease severity,¹³ and elevated oligomers were found in the CSF of subjects with AD.¹⁴ Conflicting hypotheses have been proposed that $A\beta$ is not the main reason for pathology but is just the trace of other neurodegenerative events.¹⁵ Moreover, soluble $A\beta$ may regulate memory functions by modulating synaptic plasticity at picomolar range from 20 to about 300 pM.¹⁶ Nevertheless, researchers concur that $A\beta$ seems to be an

¹InSysBio, Moscow, Russia; ²Pfizer, Cambridge, MA, USA; ³Pfizer, Groton, CT, USA. *Correspondence: T Karelina (karelina@insysbio.ru)
Received 27 January 2017; accepted 24 August 2017; published online on 28 September 2017. doi:10.1002/psp4.12249

important link in progression of AD pathology, an appropriate diagnostic biomarker and pharmacological target for treatment.¹⁷

Treatment options targeting amyloid clearance or production are under study.¹⁸ These therapies lead to the attenuation of cognitive decline in nonclinical studies,¹⁹ but have not shown significant benefit in clinical trials and have caused intolerable side effects in some cases.¹⁸ The relationship between soluble and insoluble $A\beta$ depends on formation of polymerization seeds, rates of aggregation, and fibril breakage,^{20–22} and the rate of destruction of mature fibrils.^{22,23} The aggregation of amyloid depends nonlinearly on the concentration of the soluble or free $A\beta$, which, in turn, depends on the production, degradation, and distribution between different compartments.

The detailed $A\beta$ distribution kinetics and drug effect on the brain soluble and insoluble $A\beta$ are explored only in nonclinical studies. Translation from the nonclinical species to humans requires estimation of the level of the similarity and difference between nonclinical AD models (primarily transgenic mouse models) and AD pathophysiology on a mechanistic level.

Prediction of specific mechanistic effects (through therapeutic targets) and clinical trial design optimization may be facilitated by a mechanistic model taking into account the aforementioned features. Human data should be used for verification, which was not done in existing models of amyloid accumulation.^{21,24,25}

In this analysis, a quantitative description of $A\beta$ aggregation was developed and integrated with pre-existing distribution model²⁶ to describe longitudinal changes of soluble and insoluble $A\beta$ both for healthy subjects and subjects with AD. The model would allow for exploration into how the levels of brain $A\beta$ are modified due to the changes in $A\beta$ production, clearance, or other related processes during pathology or therapeutic interventions. It can be the basis for exploration of biomarker behavior and for prediction into clinical trials. Other hallmarks of AD pathology exist (e.g., neurofibrillary tau tangles, oxidative or inflammatory markers), many of which interact with $A\beta$. Two major variants of the empirical connection between cognition and amyloid are considered: (1) neurotoxicity (loss of function and apoptosis) is directly dependent on amyloid; and (2) pathological neurodegenerative process develops independently after $A\beta$ achieves some threshold. Additionally, this model provides the ability to analyze key differences between the Tg2576 mouse AD model and human biology to make conclusions about the translation from preclinical studies into human disease understanding.

METHODS

Model structure

Two forms of $A\beta$ (only key species participating in aggregation, $A\beta_{40}$ and $A\beta_{42}$) are considered in the model. The model of $A\beta$ distribution is described in detail in ref. 26. It was extended by the addition of oligomerization and aggregation processes, as well as degradation of insoluble forms, which are presented in brain cells (BCs) and BIF (**Figure 1**). Differential equations for the aggregated amyloid have been

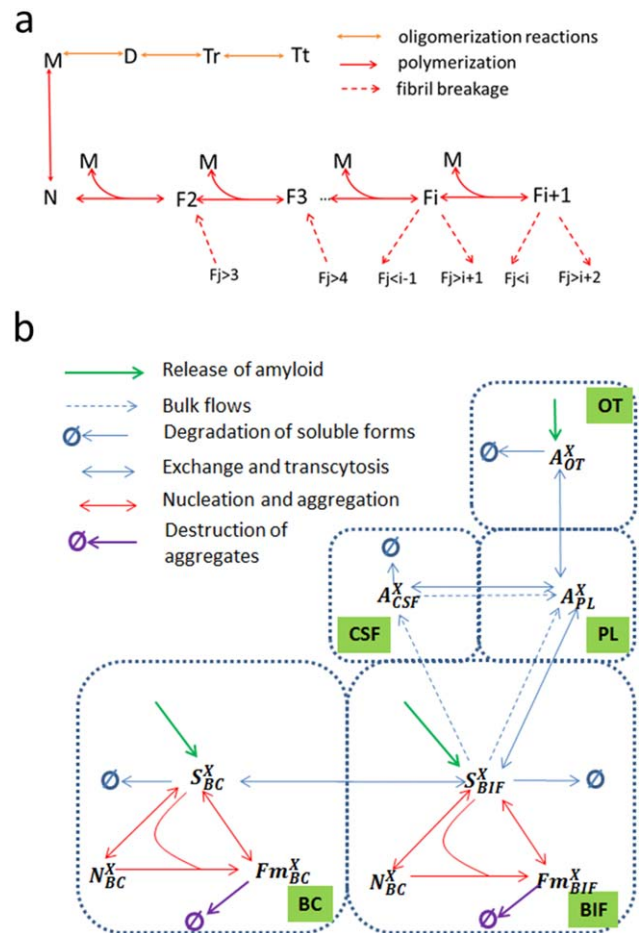


Figure 1 Sketch scheme of the model. (a) Description of the elementary processes of the polymerization and oligomerization model before reduction. Designations: D, dimers; M, monomers of amyloid beta ($A\beta$); N, nuclei; P_i , fibril of i -th length; Tr, trimers; Tt, tetramers. (b) Sketch of the processes in different compartments described in the model. The red arrows show the simplified scheme of the reduced aggregation model (see part A of the **Supplementary** for details). Compartments: BC, brain cells; BIF, brain interstitial fluid; CSF, cerebrospinal fluid; OT, other tissues; PL, – plasma.

derived in analogy with the standard approach for the polymerization description.^{20–22} The full explanation of the model is given in the **Supplementary Figure S1**. Model development and calibration stages are described in **Table 1**.

Model for longitudinal changes

Different hypotheses for $A\beta$ accumulation in sporadic AD, depending on age, have been accounted for in the model: the decrease of $A\beta$ clearance,^{27–29} shift of $A\beta_{40}$ and $A\beta_{42}$ production in the brain,^{30,31} raise of nucleation,³² and the downfall of insoluble $A\beta$ destruction.^{33,34} They are described empirically as explicit time dependence of corresponding rate constants P_i with baseline values $P_{i(\text{baseline})}$ until 60 years:

$$P_i = P_{i(\text{baseline})} \cdot (1 + A_i \cdot \text{Age}_{\text{dep}}), \quad (1)$$

Table 1 Stages of model fitting and validation using different datasets

#	Description	Parameters fitted	Data used	No. of data points	
				Fitting	EV
F0	Parameters taken from distribution model	Distribution parameters	See ref. 26	-/-	-/-
F1	Fitting of parameters for subjects with AD using integrated model	Parameters of age dependence function (manually) (3)	1) Soluble and insoluble Aβ in BR, Aβ in CSF, and PL for AD >60 years and healthy <60 years	29 (+4 +100 ^b) ^a	0
		Aβ release, aggregation, and longitudinal change (20)	2) PiB-PET data for AD	0	83
F2	Fitting of parameters for HS, choice of the best model	Longitudinal parameters (12 different variants from 1–5 parameters)	1) Soluble and insoluble Aβ in BR for HS	10 +250 ^b	0
			2) CSF for HS (OFV, AIC)	0	171 ^b
			3) PiB-PET for HS	0	527
F3	Translation of the model to Tg2576 mouse	Parameters of Age-dep function (manually) (3)	Qualitative view of the temporal characteristics of the dataset	-	0
		Release scaling factors (4)	Soluble and insoluble in BR, Aβ in CSF and PL before 6 months	10	0
		Longitudinal parameters (2)	Soluble and insoluble in BR, Aβ in CSF, and PL	70	0
F4	Translation of the model to WT mouse	Release scaling factors (3)	Steady-state data for soluble and insoluble Aβ in BR, Aβ in CSF, and PL	4	0

Aβ, amyloid beta; AD, Alzheimer disease; Age-dep, age-dependent; AIC, Akaike information criterion; BR, brain; CSF, cerebrospinal fluid; EV, external verification (comparison of data with predictions); HS, healthy subjects; OFV, objective function value; PET, positron emission tomography; PiB, Pittsburgh compound B; PL, plasma; WT, wild-type.

^aData from healthy population (before 60 years of age) used during fitting of AD; ^bData for fitting (validation) transformed to medians.

where

$$Age_{dep} = 1 - \frac{1}{1 + K_{time} \cdot \exp((prog \cdot (t - t_{decline})))} \quad (2)$$

with specific coefficients (amplitudes, A_i) for each process hypothesized to contribute to the pathology (parameter of the model). Here, K_{time} , $prog$, and $t_{decline}$ are parameters of the curve, and t is the time in years.

Description of the Aβ influence on cognition

The Aβ toxicity was described under simplifying assumptions: (1) the brain soluble $A\beta_{42}$ (monomer and soluble oligomers) is the key toxic form; (2) simple linear models were chosen as the cognition dataset is sparse, thereby limiting additional assumptions on model structure; (3) there are no irreversible changes, thus, a decrease in $A\beta_{42}$ would lead to an immediate recovery of cognitive function; and (4) parameters have been chosen empirically to achieve gradual change of the Adas-cog score from 8 to $\sim 35^{11}$ during the overall disease progression.

A potential physiological function of $A\beta_{42}$ at low concentrations is also considered in the model.¹⁶

The cognitive status depends on the quantity of the non-degenerated neurons (N) and on their functional capacity ($fsol$):

$$Cogn \sim N \cdot fsol \quad (3)$$

where N decreases with $A\beta_{42}$ accumulation and $fsol$ may decrease with $A\beta_{42}$ depletion. In this case, change of cognition can be described as:

$$\Delta Adas_{cog} = coef \cdot (1 - fsol(A\beta_{42}) + tox(A\beta_{42}) \cdot fsol(A\beta_{42})) \quad (4)$$

Considered toxicity hypotheses expressed as $tox(A\beta_{42})$ are shown in **Table 2** and described in detail in the **Supplementary Information**, as well as derivation of function $fsol(A\beta_{42})$.

Mechanism-specific simulations

Simulations for specific mechanistic targets, amyloid release inhibition (RI) and destruction of insoluble amyloid (DT), were performed in different regimens: corresponding parameter of a target process (release rate constant or destruction rate constant) was multiplied on the function of the drug effect EFF :

$$EFF = 1 - K_{inh}, \quad (5)$$

for the constant therapeutic intervention, termed a “cutting regimen” (CR), or:

$$EFF = 1 - K_{inh} \cdot Age_{dep} \quad (6)$$

for adaptive, or a “progressive regimen” (PR), with therapeutic intervention increasing gradually to compensate for the pathological change of corresponding parameter (see paragraph two of the Methods section). Therapy influenced equally $A\beta_{42}$ and $A\beta_{40}$ forms. To test the toxicity hypotheses, simulated mechanistic intervention (simulated therapy) was switched on at 70 (preclinical) and 75 years (mild AD), which are the approximate ages of cognitive symptom manifestations for sporadic cases.

Table 2 Hypotheses of the amyloid toxicity.

A β toxicity hypothesis	A β is required ^a	#	Comments	P value for rejection of hypothesis based on datasets				
				1	2	3	4	5
Proportional	No	1.1	$tox(A\beta_{42}) = K_{dr} \cdot (Asoluble_{BR}^{A\beta_{42}} - base_{health})$, $base_{health} = 1$ nM	< 0.001	< 0.001	< 0.001	< 0.001	1
	Yes	2.1	Same as 1.1, but takes into account decrease of cognition for the low Ab_{42} levels	1	1	1	1	1
Threshold	No	1.2	$tox(A\beta_{42}) = K_{thr} * (t - t_{st})$ if $Asoluble_{BR}^{A\beta_{42}} > base_{health}$	< 0.001	< 0.001	< 0.001	< 0.001	1
	Yes	2.2	Same as 1.2, but takes into account decrease of cognition for the low Ab_{42} levels	1	1	1	1	1
Proportional and threshold	No	1.3	Combination of 1.1 and 1.2	0.2561	< 0.001	0.1116	< 0.001	1

Simulations using hypotheses have been considered with data (simulations based on data mean and SD) using Wilcoxon one-side criterion for unpaired observations. The null hypothesis was that model overestimates treatment effect (Adas-cog difference) not higher than by 1 point. Datasets: Adas-cog from avagacestat data set (Coric *et al.*,³⁹ 2012): 1–50 mg, 12 weeks, 2–125 mg, 12 weeks, 3–50 mg, 24 weeks, 4–125 mg, 24 weeks; bapineuzumab data (Rinne *et al.*,⁴⁰ 2010), Adas-cog for 78 weeks.

A β , amyloid beta.

^aHypothesis accounts for positive influence of A β on neuronal functioning.

Statistical analysis

A one-sided nonparametric (Wilcoxon) test for unpaired observations was used to compare simulations based on hypotheses with clinical trials. Observations were simulated using mean and SD from publications. To note, due to assumption (3) of the A β influence on cognition, the model predicts the most optimistic scenario, tending to overestimate the treatment effect. Software R, version 3.2, was used for all statistical procedures.

RESULTS

Description of patients with AD data

The model sufficiently characterized $A\beta_{42}$ and $A\beta_{40}$ data in patients with AD (**Figure 2a**, **Supplementary Figures S5 and S6**), the medians of the data are within the model prediction bands for the observed medians. The CSF $A\beta_{42}$ before 60 years is not well captured by the model, because age <60 years is not attributed to sporadic AD, as considered in this model. The model predicts a decrease of CSF $A\beta_{42}$ vs. healthy baseline after 60 years (**Figure 2a**, **upper panel**), which is not observed for $A\beta_{40}$ (**Supplementary Figure S5**). Destruction of insoluble amyloid (**Supplementary Figure S2**) and $A\beta_{42}$ production rate have the greatest amplitude of longitudinal change among considered processes (**Supplementary Table S3**). The decrease of the insoluble amyloid degradation rate constant during AD in the model is consistent with microglial phagocytosis descent.²³ Plasma A β increase (**Supplementary Figure S7**) is mainly determined by the decline in the A β clearance with the minimal contribution from the brain processes.²⁶ The model was verified using independent PET DVR dataset for subjects with AD (**Figure 2b**, **left panel**).

Description of the healthy subject data

Different variants of parameter sets were explored to describe the healthy subject data (**Supplementary Table S2**). This exploration revealed key factors distinguishing healthy subjects and subjects with AD. Recalibration of the progression rate for healthy subjects (**Supplementary Table S2**, H14)

allowed for the adequate description of the data used for fitting and verification (CSF data on **Figure 2a**). Although there is significant variability across healthy subject DVR data, the 95% confidence band for model prediction contains the median of the healthy subject data (**Figure 2b**, **right panel**). The BIF soluble $A\beta_{42}$ goes down (**Supplementary Figure S10**) in subjects with AD, coinciding with decrease in CSF. The BIF $A\beta_{42}$ concentration in healthy subjects is not lower than 0.01 nM and BC soluble $A\beta_{42}$ concentration does not exceed 1 nM across multiple variants of the model parameterization. This is in contrast to subjects with AD, whereas BIF $A\beta_{42}$ decreases, whereas BC A β increases. The BIF amyloid concentration of 0.01 nM is close to the lower limit of positive LTP regulation from *in vitro* experiments.¹⁶ Insoluble $A\beta_{42}$ and $A\beta_{40}$ concentrations change similarly in healthy and AD populations, but, unlike in the AD population, the simulated confidence band for the healthy individuals does not exceed concentration of 300 nM, corresponding to the threshold value of amyloid burden detection.³⁵ This model variant under predicts part of the data for soluble and insoluble amyloid, but adequately describes the independent dataset on CSF $A\beta_{42}$ and $A\beta_{40}$ concentrations used for validation.

Other models (**Supplementary Table S2**, **Supplementary Figure S10**) predict multiple variants of amyloid behavior in the BIF and BC of healthy subjects. Some models describe higher levels of soluble $A\beta_{42}$ (**Supplementary Figure S10**) and demonstrate better values of the fitting criteria (**Supplementary Table S2**). Model H14 was chosen due to its simplicity and the very good validation ratio. It may represent a healthy population, which also moves toward the AD state but at a very low rate. Plasma data were used neither for fitting nor for external verification of the model for healthy subjects as there is no difference between healthy and AD data,³⁶ and plasma has minimal influence on the brain amyloid.²⁶ The amplitude of the amyloid clearance decrease was assumed to be the same for both groups. Based on the model output, the decrease of plasma A β by 80% does not change the concentration of the brain A β forms (**Supplementary Figure S13**).

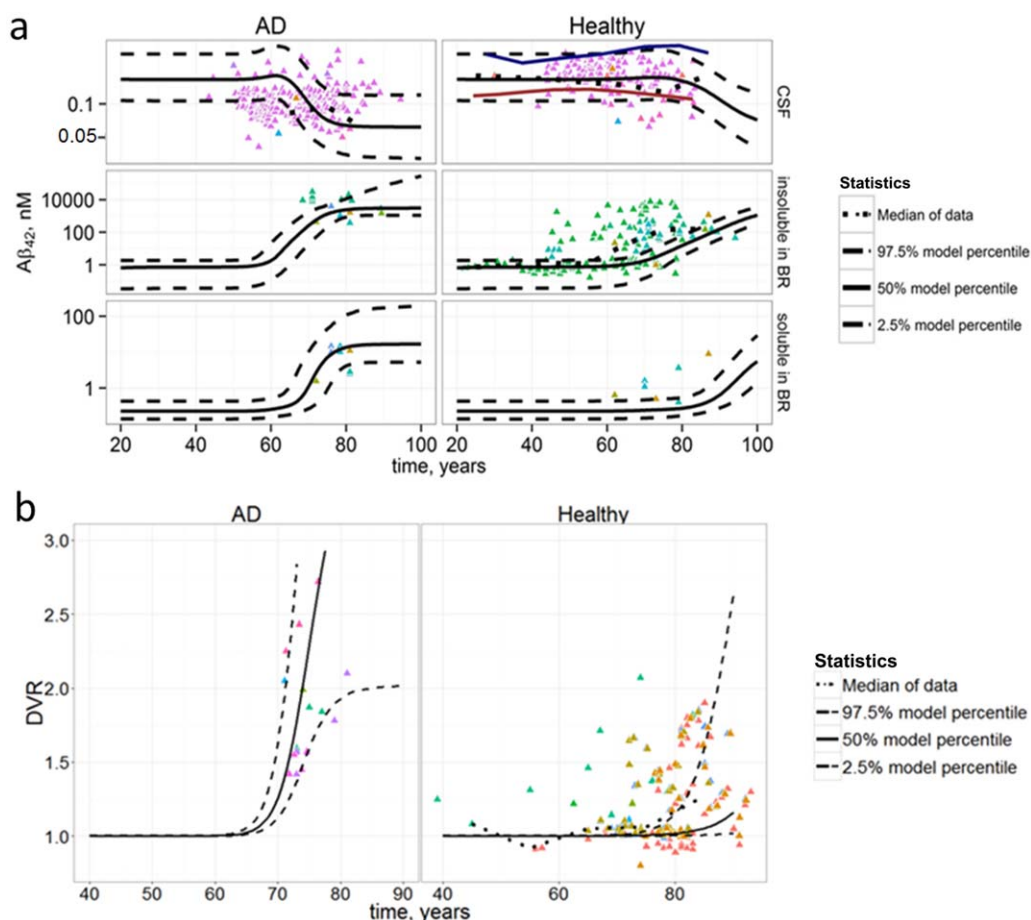


Figure 2 Model calibration and performance. (a) Results of the fitting of the Alzheimer disease (AD; left) individuals and healthy (right) individuals with 95% confidential bands for uncertainty of model parameters. For the healthy individuals, results from the model with a single parameter recalibration (see **Supplementary Table S2, H14**) are shown. The blue and red line lines (upper right) correspond to least square analysis from published sources. Median amyloid beta ($A\beta$) in cerebrospinal fluid (CSF) for AD (upper left) was taken only for points after 60 years. (b) Verification of the model for AD (left) and healthy (right) individuals by the positron emission tomography (PET) DVR data from different sources with confidence bands for model predictions determined by uncertainty of parameters. For verification, we chose data from cortex and hippocampus with cerebellum used as reference region for PiB binding estimation. Colors denote different data sources (see complete reference list in **Supplementary Figures S6–S9**). All y-scales are \log_{10} -scales. BR, brain.

Translation of the model from human to the mouse Tg2576 and wild type mouse

The final human model parameters were used to describe amyloid accumulation over the rodent lifespan. The amyloid synthesis parameters and longitudinal effect parameters were recalibrated to allow for the satisfactory description of the rodent data (**Supplementary Figures S11 and S12**).

Simulations of therapy

The decrease in insoluble $A\beta_{42}$ accumulation (**Figure 3a, bottom panel**) during the RI therapy is preceded by an abrupt decrease of soluble $A\beta_{42}$ (**Figure 3**) below physiological range. Transgenic mouse simulation results are similar, but BC $A\beta_{42}$ concentration is still higher than for the wild type mouse, and insoluble $A\beta_{42}$ does not decrease from baseline. Destruction therapy leads to the increase of the soluble forms of $A\beta_{42}$ in BIF both in human and mouse models (**Figure 3, middle row**). Time when an intervention is initiated (prevention at 60 years or treatment at 75 years) does not influence

the new amyloid steady-state level or time of its achievement: therapy with early start and the late therapy lead to the same state at ~ 75 – 80 years. Steady state is determined by the intrinsic time of disease progression and intervention type. Although BIF soluble $A\beta_{42}$ concentration increases during DT, BC $A\beta_{42}$ level decrease when compared to the AD placebo (for preclinical AD such effect appears after 10 years). To note, this effect was not predicted in the mouse model.

Attenuating soluble amyloid in the brain 10 times below normal levels resulted in insoluble $A\beta_{42}$ levels higher than normal after 10 years (**Figure 3a, bottom panel**). A large inhibition of $A\beta$ production (CR) before disease progression (prevention targeted treatment) leads to almost zero difference in BIF $A\beta_{42}$ concentrations vs. AD placebo after 10 years of therapy (**Figure 3a, middle, left panels**), although BC $A\beta_{42}$ and insoluble amyloid differ significantly from placebo (**Figure 3a, top and bottom, left panels**).

The magnitude of “progressive” therapy depends on the degeneration stage of the system and, thus, makes effect

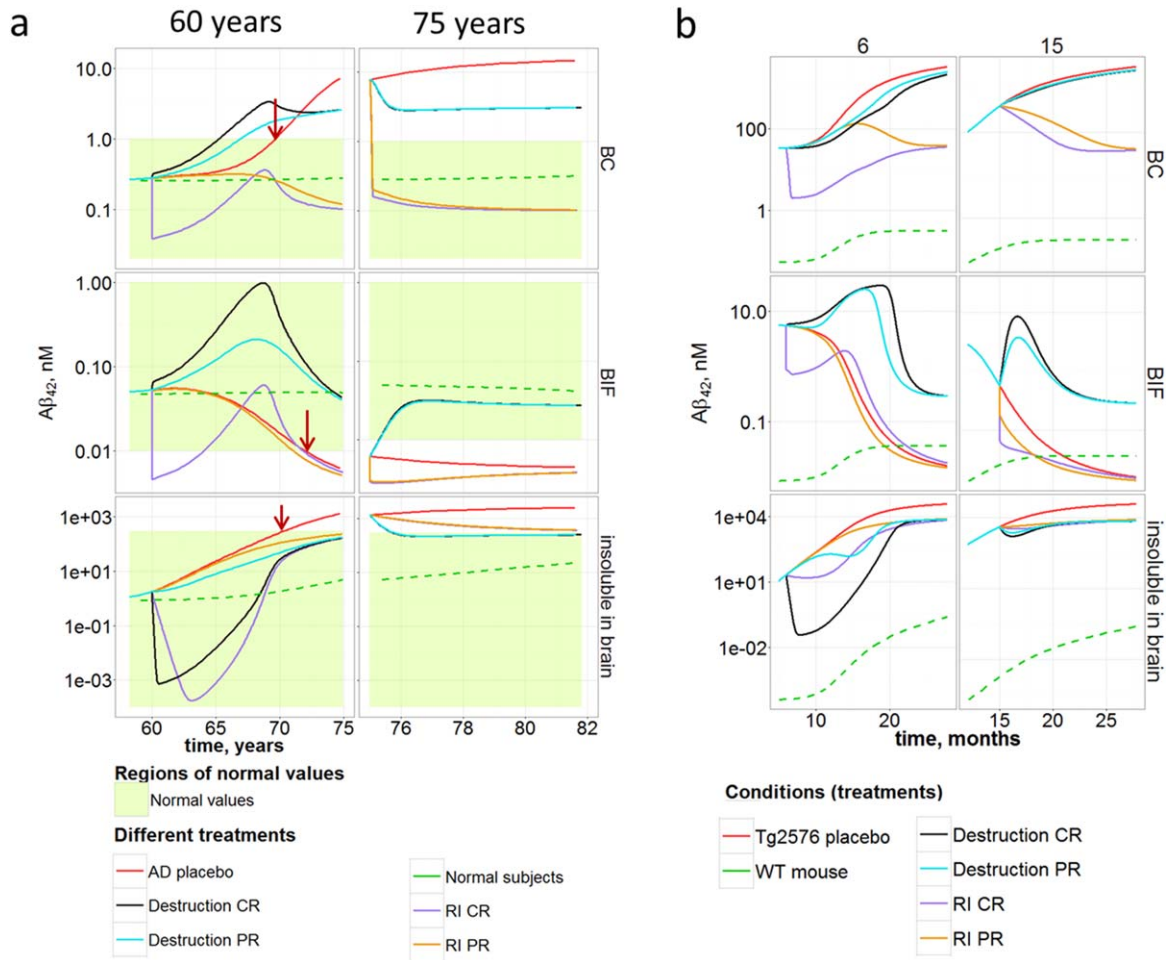


Figure 3 Simulation of different types of treatment (inhibition of production by 80% maximally and activation of destruction of plaques to 600%) for subjects with Alzheimer disease (a) and Tg2576 mouse (b) according to “cutting regime” (CR) and “progressive regime” (PR). For PR, the maximal value of therapeutic intervention is the same as for the CR, age-dependence parameters are the same as for the disease progression description (see Methods and **Supplementary Table S3**). Therapy simulations are compared with levels of normal values (light green area on a) and the model forecasted trajectory for normal subjects (dashed green line). Red arrows indicate the time at which the biomarker was no longer contained in the region of normal values (a). Two ages of therapy start were used for humans: 60 years (left) and 75 years (right). Black and cyan lines are overlapping on the right column panels, predicting absence of difference for two regimens of DT at this stage, the same for release inhibition (RI; orange and violet). (b) Two ages of therapy start were used for the mouse models: 6 months (left) and 15 months (right). Comparison with the wild-type (WT) mouse (green dashed line) is given (b). A β , amyloid beta; BC, brain cell; BIF, brain interstitial fluid.

on the system less radical with fewer declines from the healthy physiological state. DT (PR) with titration from zero at 60 years to 600% at 80 years (**Figure 3, left panel**) yields much lower growth of soluble A β_{42} in BIF than CR (“cutting” therapy) causes. Such preventive therapy makes sense only at the early stage of the disease, when levels of the most of the biomarkers are indistinguishable from control.

Testing the hypotheses of A β toxicity

The Adas-cog model performed satisfactorily on collected data (**Supplementary D and Figures S14 and S15**). All hypotheses allow for approximate description of AD progression (**Supplementary Figure S15**). Models predict that starting from the value about 20 Adas-cog will change by ~5 point score during the next 2 years, which is similar to

the estimates reported in the literature.^{37,38} Each targeted mechanism (RI or DT) shows differing trajectories depending on the disease severity (**Figure 4**). For the preclinical AD simulations, minimal effect, as compared to placebo, would be expected for ~2 years, but a change in the biomarker could be observed earlier. The simulations for the mild AD population suggest a more rapid therapeutic effect depending on the hypothesized toxicity. Here, A β production inhibition as a possible therapy would yield a more rapid effect if the toxicity follows the proportional or threshold model, but the effect is negated if a minimal concentration of A β_{42} is required for neuronal function. Threshold hypotheses predict no positive effect unless inhibition is high enough to drop A β_{42} below the toxic threshold (50% inhibition), then during the first month of treatment a large (5–10) point difference would be expected. If amyloid is functionally important

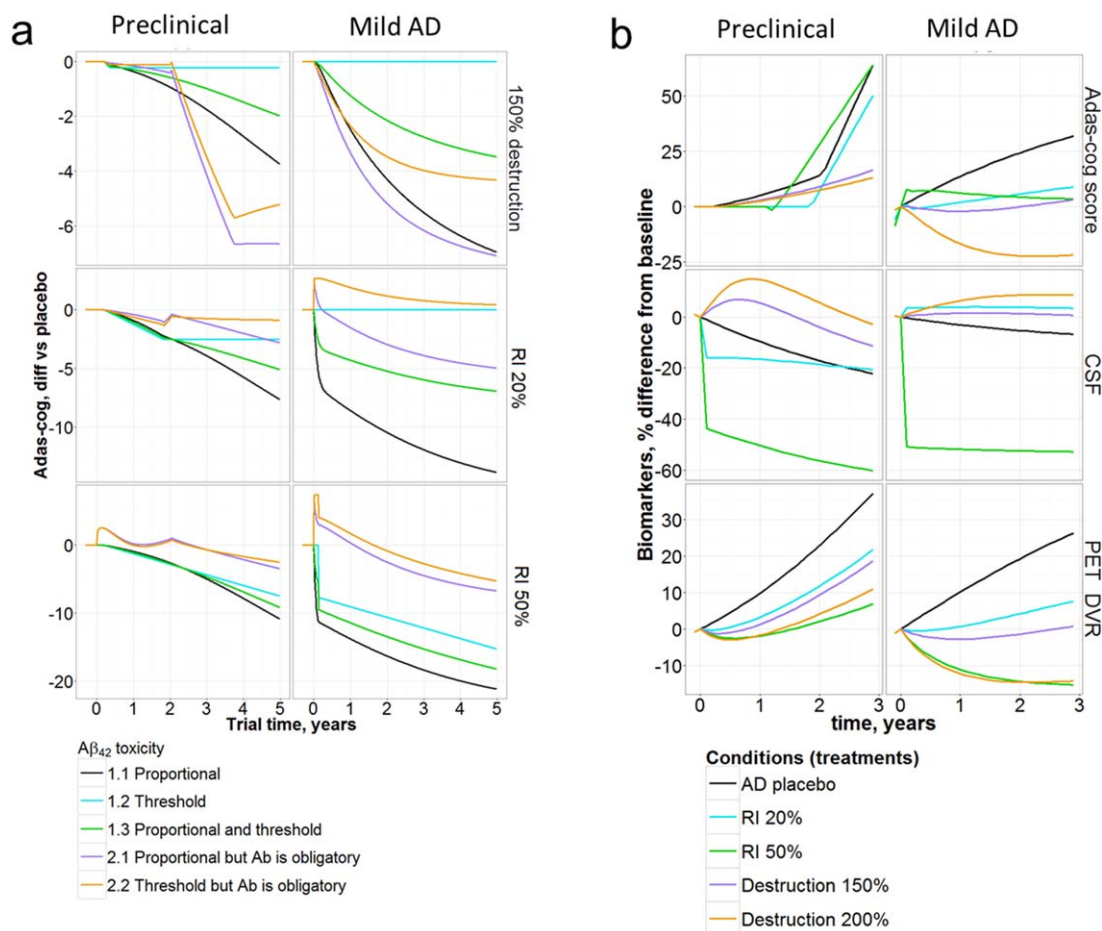


Figure 4 Effect of different therapies on cognitive function and other biomarkers under different hypotheses of amyloid toxicity (see **Table 2**). Two variants of therapy initiation were applied: preclinical stage (70 years, left) and mild Alzheimer disease (AD) stage (75 years, right). **(a)** Amyloid beta ($A\beta$) toxicity influencing cognitive outcomes (Adas-cog) simulations under different hypotheses. **(b)** Influence of different treatments on the cognitive function, cerebrospinal fluid (CSF) amyloid and positron emission tomography (PET) DVR with respect to baseline under hypothesis 2.1 (**Table 2**). Ab, amyloid 42; RI, release inhibition.

(hypotheses 2.1 and 2.2 of **Table 2**), then an initial cognitive decline would be expected for more intense RI therapy (simulated at 50% inhibition). This apparent deterioration would be expected to decline over time leading to a net improvement over 5 years. No negative effect is predicted at low level of destruction activation for any of the hypotheses.

Simulated CSF $A\beta_{42}$ dynamics differ between AD populations (**Figure 4b**). No decrease of PET DVR vs. baseline is predicted with any of the proposed therapies in the preclinical AD population, although the difference from placebo is expected to grow with time. For the mild AD simulation, a 200% increase of $A\beta$ destruction is expected to cause a 15% DVR decrease as compared to baseline within 2 years (**Figure 4b, bottom right panel**) as well as cognitive improvement by ~20%, compared to baseline (as predicted by hypothesis 2.1). Simulated CSF $A\beta_{42}$ concentration change vs. baseline is small (increase by 2–10%) for mild AD group and seems to be nonmonotonic for preclinical AD (**Figure 4b, middle left panel**).

We simulated avagacestat clinical trial data,³⁹ applying levels of 20% and 50% production inhibition, corresponding to

CSF $A\beta_{42}$ inhibition observed at doses 50 and 125 mg, respectively. Validity of each hypothesis was tested by the calculation of *P* value for the difference between data and model predictions. As our model predictions tend to be optimistic due to assumptions (see Methods), the null hypothesis for each test was taken as absence of significant overprediction (more than 1 point), instead of simple coincidence of predictions vs. observations. Hypotheses without $A\beta_{42}$ -positive influence (**Table 2, 1.1–3**) can be rejected as they overestimate treatment effect (*P* value < 0.001). Hypotheses 2.1 and 2.2 cannot be rejected (*P* value = 1 in **Table 2**), and simulations under these hypotheses are more or less close to the results of the trial (**Figure 5**), predicting probability of cognitive decline for higher doses. The simulations for DT (increase to 150%) under toxicity hypotheses 2.1 and 2.2 are similar to the observed results of the bapineuzumab study⁴⁰ (**Supplementary Figure S14**), which show about 15% DVR decrease at 78 weeks (**Figure 4b, bottom right panel**). In contrast to avagacestat data, the bapineuzumab trial results do not allow for rejection of any hypotheses.

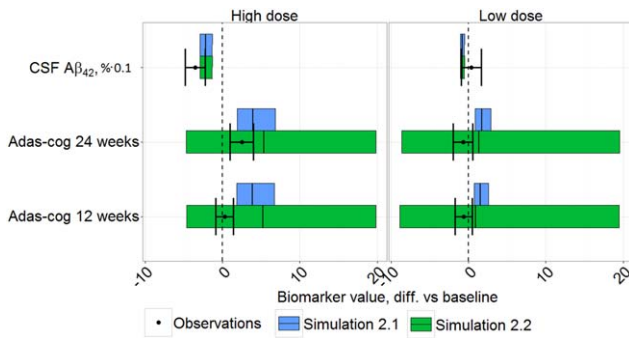


Figure 5 Comparison of results of amyloid beta ($A\beta$) toxicity influencing cognitive outcomes (Adas-cog) simulation by hypotheses 2.1 and 2.2 and results of avagacestat clinical trial.³⁹ Different doses of avagacestat were given to patients of about 75 years of age, and cerebrospinal fluid (CSF) changes vs. baseline at 24 weeks and Adas-cog score changes at 12 and 24 weeks with respect to baseline were measured. Confidence intervals for simulation calculated through the uncertainty of the aggregation and longitudinal parameters. Adas-cog change from baseline (points) and for CSF ($A\beta_{42}\%$ change from baseline $\cdot 10^{-1}$) are displayed. For observations, SD is shown.

DISCUSSION

The model presented here describes the accumulation of $A\beta$ in the brain and longitudinal changes in other compartments for human, healthy individuals, patients with AD, and transgenic mice Tg2576. It was constructed mechanistically, calibrated, and verified on a large number of clinical and animal data.

Our model provides a unique possibility to explore the differences between healthy subjects and subjects with AD in terms of quantities that are difficult to be measured, $A\beta$ concentrations in BIF, and BC, which may differentially contribute to toxic mechanisms, and CSF biomarkers. Concentrations of insoluble brain $A\beta$ and soluble $A\beta_{42}$ in BC exceed $1\ \mu\text{M}$ and $1\ \text{nM}$, respectively, in the AD population, and remain below these levels in healthy subjects. Soluble $A\beta_{42}$ in the BIF of subjects with AD falls to subphysiological levels due to aggregation (**Figure 3a, middle panel**). It may raise the question whether the plaques themselves, or even oligomers, are the main contributors into the neuron pathology. For example, depletion of $A\beta_{42}$ soluble pool due to its absorbance to plaques may lead to the loss of positive function observed for the picomolar $A\beta_{42}$.⁴¹ In addition, activity-dependent modulation of endogenous $A\beta$ may normally participate in a negative feedback keeping neuronal hyperactivity in check.⁴² One of the therapeutic options may be to stabilize $A\beta$ levels close to a physiologically relevant value. Plaque destruction increase (to 600%) would be able to normalize insoluble $A\beta$ (to about 300 nM) in brain and soluble $A\beta$ in BIF during 1 year. Potentially after such stabilization of plaques, additional inhibitory therapy could be applied to decrease brain $A\beta$. The CSF $A\beta_{42}$ would be a sufficient biomarker for such a treatment and should neither exceed the control level nor significantly fall down, whereas PET-PiB binding should decrease.

Model predicts that the main reason of $A\beta$ accumulation is a failure of insoluble $A\beta$ destruction. Although destruction processes, such as enzyme proteolysis, astrocyte, and microglial phagocytosis, are not described mechanistically in our model, many hypotheses exist that the breakdown of these processes may be the driving force for aging,⁴³ and, thus, the model insight seems reasonable. To note, this model was constructed to describe the sporadic AD population, therefore, populations with APP mutations are to be described by the shifts in production, degradation, polymerization, and oligomerization parameters.

Transgenic mouse data were fitted by parameters of the release and $A\beta_{40}$ polymerization. This presumably may reflect already observed distinct physical and chemical properties of peptides generated in the mouse AD model.⁴⁴

Soluble $A\beta_{42}$ in Tg2576 will not decrease below physiological levels corresponding to wild-type mice until 2–3 months of the treatment. This is expected as the initial concentrations and production of amyloid in Tg2576 strongly exceeds those in the wild-type mouse.⁴⁵

Only several designs may be used for actual confirmation or rejection of $A\beta$ toxicity hypotheses (**Figure 4a, Table 2**). Nevertheless, outcomes of other designs may still inform about particular properties of the system. For example, positive clinical outcomes (Adas-cog decrease) at light inhibition may suggest that $A\beta$ inputs in degeneration as a primary driver of disease, whereas negative results at low RI would attest in favor of threshold (or prion-type) hypothesis.

Initiation of early therapy (**Figure 4a, left panel**) would not be expected to demonstrate any differences vs. placebo for the first 2 years. In this preclinical AD group (in the model), cognition is still very close to normal, but soluble and insoluble $A\beta_{42}$ leave the region of normal values (**Figure 3, left panel**). The BIF soluble $A\beta_{42}$ leaves the normal region at 72 years in the preclinical AD group according to the model, that is why hypotheses 2.1 and 2.2 (**Table 2**) forecast no difference between treatment and placebo for over 2 years. The main limiting assumption of our hypotheses is the absence of irreversible toxicity or long-term cellular processes. They significantly overestimate pharmacodynamic outcomes predicting almost 20 points of Adas-cog improvement, which means complete healing. These and other additional hypotheses could be explored using this model and new emerging datasets at a future time. Soluble and insoluble $A\beta_{42}$ dynamics are qualitatively similar in AD (**Figure 3a, upper and bottom rows**) and leave the region of normal values simultaneously (70 years), so toxicity descriptions, in terms of dependence on soluble (in brain cells) or insoluble forms, may be similar.

Even one chosen hypothesis 2.1 (**Figure 4b**) predicts the diversity of biomarker and clinical outcome behavior depending on the treatment protocol. For example, 50% RI leading to 50% CSF $A\beta$ decline for both preclinical and mild AD causes distinct behaviors of other biomarkers: for the preclinical AD population (**Figure 4b**) after 2 years of therapy, the model predicts neither difference from baseline in DVR nor Adas-cog. In the mild AD case, 50% RI corresponds with much greater responses of DVR, and potential decline of Adas-cog vs. placebo with time.

Responses predicted by simulation for the hypothesis 2.1–2.2., but not the other hypotheses, are qualitatively

similar to results obtained in avagacestat clinical trial,³⁹ as well as the bapineuzumab study.⁴⁰ This would suggest that hypotheses of $A\beta$ impact on cognition can be tested. The trend for a decrease in cognition in the avagacestat (and semagacestat⁴⁶) trial would also bolster the concerns given hypotheses 2.1 and 2.2, in which cognition may be impaired if $A\beta$ concentrations were altered to subphysiological levels. Additionally, if one were to extrapolate from **Figure 4a**, hypotheses 2.1 and 2.2 may be tested when $A\beta$ production is inhibited >50% over a shorter duration trial (<1 year). In this case, the predictions do not correspond to observation at 12 weeks, in which no cognitive decline is reported in the clinic (**Figure 5**). This may be due to model misspecification in the longitudinal nature of the low $A\beta$ levels, other protein/macro molecules compensating for lower $A\beta$, or that the *in vitro* findings do not translate into the *in vivo* setting. Other adverse events may be related to GS inhibition but are not captured in this model. Results presented here do not deal with all possible hypotheses (e.g., we did not consider insoluble or oligomeric amyloid toxicity), nor do we show the extremes of $A\beta$ inhibition (~100% inhibition) or degradation, as neither consider specific features of different population (based, e.g., on ApoE genotype), but we have used this model and subsequent simulations to illustrate the approach of applying quantitative systems pharmacology (QSP) models for the purpose of hypothesis testing.

CONCLUSIONS

The constructed mechanistic model, verified with a number of data, allows insights into different aspects of translational and clinical studies and reveals key features, distinguishing healthy and AD populations. Physiological ranges and results of *in vitro* studies analyzed in this article suggest the possible benefit achieved by maintaining physiologic concentrations of different amyloid species. The model allows for the simulation of such appropriate regimens and may also be used for exploring other combination type regimens (inhibition of soluble $A\beta$ and degradation of insoluble $A\beta$) *in silico*.

Direction, magnitude, and rate of biomarker changes predicted by the model provide the basis for planning and analysis of ongoing trials. As clinical studies for neurodegenerative diseases become more difficult to execute (due to cost and duration), systems pharmacology tools, like the one presented here, provide a greater understanding of the actual ability of a novel study to test the underlying hypothesis.

Acknowledgments. The authors are grateful to the InSysBio team for technical and theoretical support and Aleksey Alekseev for technical support of calculations.

Conflict of Interest. T. Karelina, O. Demin Jr, and O. Demin are external consultants who were paid to do this research. T. Nicholas and S. Duvvuri are employees of Pfizer.

Author Contributions. T.K., O.D. Jr, O.D., S.D., and T.N. wrote the article. T.K., O.D., S.D., and T.N. designed the research. T.K., O.D. Jr, and O.D. performed the research. T.K., O.D. Jr, and O.D. analyzed the data.

- Selkoe, D.J. Toward a comprehensive theory for Alzheimer's disease. Hypothesis: Alzheimer's disease is caused by the cerebral accumulation and cytotoxicity of amyloid beta-protein. *Ann. NY Acad. Sci.* **924**, 17–25 (2000).
- Stine, W.B. Jr, Dahlgren, K.N., Krafft, G.A. & LaDu, M.J. In vitro characterization of conditions for amyloid-beta peptide oligomerization and fibrillogenesis. *J. Biol. Chem.* **278**, 11612–11622 (2003).
- Wang, J., Dickson, D.W., Trojanowski, J.Q. & Lee, V.M. The levels of soluble versus insoluble brain Abeta distinguish Alzheimer's disease from normal and pathologic aging. *Exp. Neurol.* **158**, 328–337 (1999).
- Fagan, A.M. et al. Inverse relation between in vivo amyloid imaging load and cerebrospinal fluid Abeta42 in humans. *Ann. Neurol.* **59**, 512–519 (2006).
- Villemagne, V.L. et al. Amyloid β deposition, neurodegeneration, and cognitive decline in sporadic Alzheimer's disease: a prospective cohort study. *Lancet Neurol.* **12**, 357–367 (2013).
- Palop, J.J. & Mucke, L. Amyloid-beta-induced neuronal dysfunction in Alzheimer's disease: from synapses toward neural networks. *Nat. Neurosci.* **13**, 812–818 (2010).
- Karran, E., Mercken, M. & De Strooper, B. The amyloid cascade hypothesis for Alzheimer's disease: an appraisal for the development of therapeutics. *Nat. Rev. Drug Discov.* **10**, 698–712 (2011).
- Götz, J., Eckert, A., Matamalas, M., Ittner, L.M. & Liu, X. Modes of $A\beta$ toxicity in Alzheimer's disease. *Cell. Mol. Life Sci.* **68**, 3359–3375 (2011).
- Dahlgren, K.N., Manelli, A.M., Stine, W.B. Jr, Baker, L.K., Krafft, G.A. & LaDu, M.J. Oligomeric and fibrillar species of amyloid-beta peptides differentially affect neuronal viability. *J. Biol. Chem.* **277**, 32046–32053 (2002).
- Wogulis, M., Wright, S., Cunningham, D., Chilcote, T., Powell, K. & Rydel, R.E. Nucleation-dependent polymerization is an essential component of amyloid-mediated neuronal cell death. *J. Neurosci.* **25**, 10711–1080 (2005).
- Rosenberg, P.B. et al. Cognition and amyloid load in Alzheimer disease imaged with florbetapir F 18(AV-45) positron emission tomography. *Am. J. Geriatr. Psychiatry* **21**, 272–278 (2013).
- Aizenstein, H.J. et al. Frequent amyloid deposition without significant cognitive impairment among the elderly. *Arch. Neurol.* **65**, 1509–1517 (2008).
- McLean, C.A. et al. Soluble pool of Abeta amyloid as a determinant of severity of neurodegeneration in Alzheimer's disease. *Ann. Neurol.* **46**, 860–866 (1999).
- Santos, A.N. et al. Amyloid- β oligomers in cerebrospinal fluid are associated with cognitive decline in patients with Alzheimer's disease. *J. Alzheimers Dis.* **29**, 171–176 (2012).
- Rottkamp, C.A., Atwood, C.S., Joseph, J.A., Nunomura, A., Perry, G. & Smith, M.A. The state versus amyloid-beta: the trial of the most wanted criminal in Alzheimer disease. *Peptides* **23**, 1333–1341 (2002).
- Puzzo, D. et al. Picomolar amyloid-beta positively modulates synaptic plasticity and memory in hippocampus. *J. Neurosci.* **28**, 14537–14545 (2008).
- Jack, C.R. Jr et al. Brain β -amyloid load approaches a plateau. *Neurology* **80**, 890–896 (2013).
- Chiang, K. & Koo, E.H. Emerging therapeutics for Alzheimer's disease. *Annu. Rev. Pharmacol. Toxicol.* **54**, 381–405 (2014).
- Comery, T.A. et al. Acute gamma-secretase inhibition improves contextual fear conditioning in the Tg2576 mouse model of Alzheimer's disease. *J. Neurosci.* **28**, 8898–8902 (2005).
- Knowles, T.P. et al. An analytical solution to the kinetics of breakable filament assembly. *Science* **326**, 1533–1537 (2009).
- Shoghi-Jadid, K. et al. Imaging beta-amyloid fibrils in Alzheimer's disease: a critical analysis through simulation of amyloid fibril polymerization. *Nucl. Med. Biol.* **32**, 337–351 (2005).
- Lee, C.C., Nayak, A., Sethuraman, A., Belfort, G. & McRae, G.J. A three-stage kinetic model of amyloid fibrillation. *Biophys. J.* **92**, 3448–3458 (2007).
- Koenigsnecht-Talboo, J. et al. Rapid microglial response around amyloid pathology after systemic anti- $A\beta$ antibody administration in PDAPP mice. *J. Neurosci.* **28**, 14156–14164 (2008).
- Craft, D.L., Wein, L.M. & Selkoe, D.J. A mathematical model of the impact of novel treatments on the A beta burden in the Alzheimer's brain, CSF and plasma. *Bull. Math. Biol.* **64**, 1011–1031 (2002).
- Parkinson, J. et al. Modeling of age-dependent amyloid accumulation and γ -secretase inhibition of soluble and insoluble $A\beta$ in a transgenic mouse model of amyloid deposition. *Pharmacol. Res. Perspect.* **1**, e00012 (2013).
- Karelina, T., Demin, O., Nicholas, T., Lu, Y., Duvvuri, S. & Barton, H.A. A translational systems pharmacology model for $A\beta$ kinetics in mouse, monkey, and human. *CPT Pharmacometrics Syst. Pharmacol.* (2017). [Epub ahead of print]
- Mawuenyega, K.G. et al. Decreased clearance of CNS beta-amyloid in Alzheimer's disease. *Science* **330**, 1774 (2010).

28. Deo, A.K. *et al.* Activity of P-glycoprotein, a β -amyloid transporter at the blood-brain barrier, is compromised in patients with mild Alzheimer disease. *J. Nucl. Med.* **55**, 1106–1111 (2014).
29. Nalivaeva, N.N., Belyaev, N.D., Kerridge, C. & Turner, A.J. Amyloid-clearing proteins and their epigenetic regulation as a therapeutic target in Alzheimer's disease. *Front. Aging Neurosci.* **6**, 235 (2014).
30. Li, R. *et al.* Amyloid beta peptide load is correlated with increased beta-secretase activity in sporadic Alzheimer's disease patients. *Proc. Natl. Acad. Sci. USA* **101**, 3632–3637 (2004).
31. Wahlster, L. *et al.* Presenilin-1 adopts pathogenic conformation in normal aging and in sporadic Alzheimer's disease. *Acta Neuropathol.* **125**, 187–199 (2013).
32. Huang, X., Atwood, C.S., Moir, R.D., Hartshorn, M.A., Tanzi, R.E. & Bush, A.I. Trace metal contamination initiates the apparent auto-aggregation, amyloidosis, and oligomerization of Alzheimer's A β peptides. *J. Biol. Inorg. Chem.* **9**, 954–960 (2004).
33. Mosher, K.I. & Wyss-Coray, T. Microglial dysfunction in brain aging and Alzheimer's disease. *Biochem. Pharmacol.* **88**, 594–604 (2014).
34. Zhao, W., Zhang, J., Davis, E.G. & Rebeck, G.W. Aging reduces glial uptake and promotes extracellular accumulation of A β from a lentiviral vector. *Front. Aging Neurosci.* **6**, 210 (2014).
35. Funato, H. *et al.* Quantitation of amyloid beta-protein (A β) in the cortex during aging and in Alzheimer's disease. *Am. J. Pathol.* **152**, 1633–1640 (1998).
36. Fukumoto, H., Tennis, M., Locascio, J.J., Hyman, B.T., Growdon, J.H. & Irizarry, M.C. Age but not diagnosis is the main predictor of plasma amyloid beta-protein levels. *Arch. Neurol.* **60**, 958–964 (2003).
37. Doraiswamy, P.M. *et al.* Florbetapir F 18 amyloid PET and 36-month cognitive decline: a prospective multicenter study. *Mol. Psychiatry* **19**, 1044–1051 (2014).
38. Samtani, M.N. *et al.* An improved model for disease progression in patients from the Alzheimer's disease neuroimaging initiative. *J. Clin. Pharmacol.* **52**, 629–644 (2012).
39. Coric, V. *et al.* Safety and tolerability of the γ -secretase inhibitor avagacestat in a phase 2 study of mild to moderate Alzheimer disease. *Arch. Neurol.* **69**, 1430–1440 (2012).
40. Rinne, J.O. *et al.* 11C-PiB PET assessment of change in fibrillar amyloid-beta load in patients with Alzheimer's disease treated with bapineuzumab: a phase 2, double-blind, placebo-controlled, ascending-dose study. *Lancet Neurol.* **9**, 363–372 (2010).
41. Garcia-Osta, A. & Alberini, C.M. Amyloid beta mediates memory formation. *Learn. Mem.* **16**, 267–272 (2009).
42. Kamenetz, F. *et al.* APP processing and synaptic function. *Neuron* **37**, 925–937 (2003).
43. Vilchez, D., Saez, I. & Dillin, A. The role of protein clearance mechanisms in organismal ageing and age-related diseases. *Nat. Commun.* **5**, 5659 (2014).
44. Kalback, W. *et al.* APP transgenic mice Tg2576 accumulate A β peptides that are distinct from the chemically modified and insoluble peptides deposited in Alzheimer's disease senile plaques. *Biochemistry* **41**, 922–928 (2002).
45. Hsiao, K. *et al.* Correlative memory deficits, A β elevation, and amyloid plaques in transgenic mice. *Science* **274**, 99–102 (1996).
46. Doody, R.S. *et al.* A phase 3 trial of semagacestat for treatment of Alzheimer's disease. *N. Engl. J. Med.* **369**, 341–350 (2013).

© 2017 The Authors CPT: Pharmacometrics & Systems Pharmacology published by Wiley Periodicals, Inc. on behalf of American Society for Clinical Pharmacology and Therapeutics. This is an open access article under the terms of the Creative Commons Attribution-NonCommercial License, which permits use, distribution and reproduction in any medium, provided the original work is properly cited and is not used for commercial purposes.

Supplementary information accompanies this paper on the *CPT: Pharmacometrics & Systems Pharmacology* website (<http://psp-journal.com>)